Available online at www.sciencedirect.com
ScienceDirect
Trans. Nonferrous Met. Soc. China 31(2021) 1729−1739
Transactions of Nonferrous Metals Society of China
www.tnmsc.cn

Strength prediction of multi-layered copper-based composites fabricated by accumulative roll bonding

P. SEIFOLLAHZADEH, Morteza ALIZADEH, M. R. ABBASI

Department of Materials Science and Engineering, Shiraz University of Technology, Modarres Blvd., 71557-13876, Shiraz, Iran

Received 4 August 2020; accepted 9 April 2021

Abstract: This work aims to evaluate the feasibility of the fabrication of nanostructured Cu/Al/Ag multi-layered composites by accumulative roll bonding (ARB), and to analyze the tensile properties and electrical conductivity of the produced composites. A theoretical model using strengthening mechanisms and some structural parameters extracted from X-ray diffraction is also developed to predict the tensile strength of the composites. It was found that by progression of ARB, the experimental and calculated tensile strengths are enhanced, reach a maximum of about 450 and 510 MPa at the fifth cycle of ARB, respectively and then are reduced. The electrical conductivity decreased slightly by increasing the number of ARB cycles at initial ARB cycles, but the decrease was intensified at the final ARB cycles. In conclusion, the merit of ARB to fabricate this type of multi-layered nanocomposites and the accuracy of the developed model to predict tensile strength were realized.

Key words: multi-layered composites; accumulative roll bonding; strength prediction; hardness; X-ray diffraction

1 Introduction

The increasing of strength accompanied by ductility in engineering components is a continual challenge for researchers. One idea for reaching this purpose is to fabricate multi-layered metal based composites [1−4]. These composites are composed of two or more metallic constituents, which may cause the improvement of strength while it is hard to obtain such improvement by the individual counterparts. High strength metals are usually used as the reinforcement in these composites to increase the strength of the metal base. For instance, copper was incorporated in an aluminum matrix, increasing the strength by 2.5 times [3].

The strength of composites, in addition to the constituents, strongly depends on fabrication technique used. There are different methods to fabricate multi-layered metal based composites, including explosive welding technique [5] and spark plasma sintering technology [6]. Compared to the mentioned methods, accumulative roll bonding (ARB) as a severe plastic deformation (SPD) is simpler way to fabricate multi-layered composites. Since it is possible to fabricate nanostructured bulk sheets by ARB, this process has the capability of being commercialized. This process consists of the sheets surface-preparation, stacking of them to each other according to the composite composition, rolling of the stacked sheets, and repetition of these steps. As materials undergo the ARB process, their microstructure and mechanical properties vary during the whole process as a result of strain accumulation [7]. At initial cycles, statistical dislocations are generated and their interaction increases the strength via strain hardening. By repeating the cycles, the dislocation density increases so that ultrafine-grained (UFG) or nanostructured grains evolve in the material. Grain

Corresponding author: Morteza ALIZADEH, Tel: +98-713-7278491, Fax: +98-713-7354520, E-mail: Alizadeh@sutech.ac.ir
DOI: 10.1016/S1003-6326(21)65611-X

refining in these stages is responsible for the strength improvement [8]. In addition to strain hardening and grain refinement, there are some other parameters which play a main role in the strength improvement of multi-layered metal based composites. These parameters are (1) the type and number of constituents, (2) the number of cycles (or number of layers), (3) the distribution of the constituent layers inside the fabricated composites and (4) the distance between the constituents interfaces [9,10].

Recently, different multi-layered composites including Cu/Al [3], Cu/Al/Cu [11], Al/Cu [12], Cu/Al/Mn [13] and Cu/Zn/Al [14,15] were fabricated by the ARB process and their strength was evaluated. For example, MAHDAVIAN et al [14] showed that the strength of Cu/Al/Zn multi-layered composites first increases and then decreases after middle cycles. However, a few studies have been reported on the strength prediction of multi-layered composites. In this work, Cu/Al/Ag multi-layered composites were fabricated by the ARB process and their tensile strength was predicted by a theoretical model based on strengthening mechanisms using structural parameters. Meanwhile, the mechanical properties and electrical conductivity of the composites were experimentally investigated.

2 Experimental

2.1 Starting materials and multi-layered composites processing

Multi-layered Cu/Al/Ag composites were produced by the ARB process using 1100 Al alloy (150 mm × 30 mm × 0.3 mm) and pure Cu alloy (150 mm × 30 mm × 0.5 mm) strips and pure silver powder (2.1 g) with the particle size of <5 μm. The chemical composition and some other properties of the starting materials are listed in Table 1.

The number, mass and dimensions of the starting materials were adjusted to create the composition of 70Cu−28Al−2Ag (vol.%). To improve the metallic bonding between the constituents, a surface preparation process was done according to the following steps:

(1) Degreasing of the strips with acetone to remove surface contaminations;

(2) Scratching the strips with a circle-shaped stainless steel brush.

Table 1 Chemical composition and some properties of starting materials

Material	Composition/ wt.%	Yield strength/ MPa	Elongation/ %	Micro-hardness (HV)
1100 Al	>99	65	39	26.3
Copper	>99.9	86	52.42	54.6
Ag powder	>99	–	–	–

The diameters of the brush and its wires were 100 and 0.3 mm, respectively. The aim of scratch brushing was work hardening of surface layers and thereby better cold welding. To avoid re-oxidation of the prepared surfaces, the time gap between surface preparation and next step was less than 10 min. The Al layers and silver powders were placed between the Cu layers, according to Fig. 1. The initial sandwich was cold-rolled immediately after preparation at room temperature without any lubrication. The reduction in thickness in this cycle was about 70%. Then, the rolled sandwich was horizontally cut into two halves, degreased, wire brushed, stacked and cold-rolled again. The thickness reduction at this step was about 50%. This process was repeated until 10 cycles. To prevent slipping due to the great compressive force applied during rolling, the stacked laminates were fastened with copper wires on two edges.

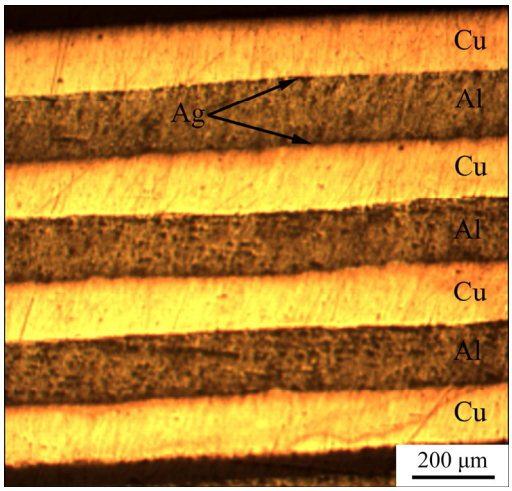

Fig. 1 Alternative layers of Cu/Al/Ag composites fabricated by ARB process

2.2 Characterization

The structural investigation of the fabricated composite specimens was conducted using X-ray

diffraction (XRD, X'pert Pro diffractometer) and scanning electron microscopy (SEM, TESCAN model) on the rolling direction−normal direction (RD−ND) plane. The diffraction angle range of 30°−80° with the step size and time of 0.05° and 3 s, respectively, was used for the XRD experiments.

Dog-bone shaped tensile samples were prepared from the fabricated composites by a wire cut machine. The gauge dimensions of the samples were 10 mm × 5 mm × 1 mm. The tensile tests were done at room temperature by an Instron machine with the strain rate of 9×10^{-4} s^{-1}. The fracture surface of the specimens was also examined by SEM. The Vickers microhardness of the layers and composites was measured on the RD−ND plane of the samples, with the load and time of 10 g and 15 s, respectively.

The electrical conductivity of the composite samples was measured by using an electrical conductivity meter in terms of % (IACS) (International Annealed Copper Standard). For the electrical conductivity measurements, the ARBed samples were machined to the dimensions of 30 mm × 10 mm × 1 mm, where the measurements were done on the transverse direction-rolling direction plane of the samples.

3 Result and discussion

3.1 Structural evaluations

Figure 2 shows the XRD pattern of the composite samples after 1, 5 and 10 cycles of ARB.

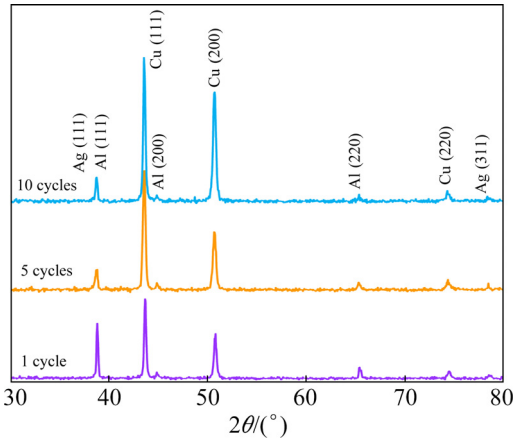

Fig. 2 XRD patterns of composite samples after 1, 5 and 10 cycles of ARB

Peaks of Cu, Al and Ag on the patterns confirm the presence of these elements in the fabricated composites. As it can be seen, no intermetallic compounds of Cu, Al and Ag elements have been created. By increasing the number of ARB cycles, a peak broadening is observed in copper and aluminum peaks, which indicates a successful grain refinement during the ARB process. It is noticeable that copper is the matrix of the fabricated composites and Al and Ag are the reinforcements. The mean crystallite size of the matrix, Cu, and reinforcement, Al, was determined by the Williamson–Hall formula as follows [16]:

$$B\cos\theta=\frac{k\lambda}{D}+4\varepsilon\sin\theta \quad (1)$$

where θ is the Bragg angle, ε is the lattice strain, λ is the X-ray wavelength, k is a constant, D is crystallite size, and B is full widths at half maximum of a diffraction peak. Crystalline (111), (200) and (220) planes were used for the determination of the mean crystallite size of the Cu matrix and (111), (200), (220) and (311) for the Al reinforcements. The Williamson–Hall plots of the Cu matrix and Al reinforcement are shown in Figs. 3(a) and 3(b), respectively.

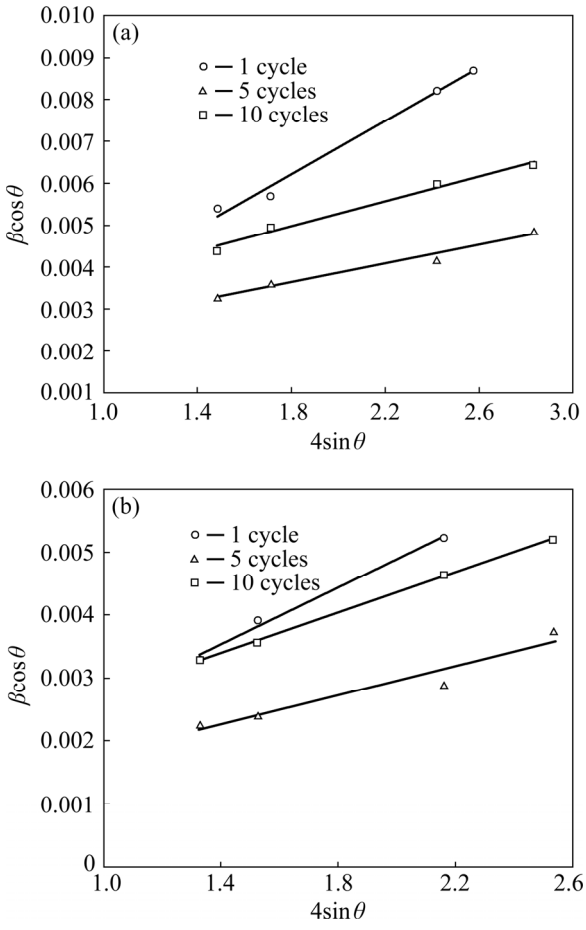

Fig. 3 Williamson–Hall plots of Cu matrix (a) and Al reinforcement (b)

Figure 4 shows the variation of the mean crystallite sizes versus the number of cycles. As it can be seen, in both Cu and Al, the mean crystallite size is decreased by increasing the ARB cycles. The comparison of the curves shows that the mean crystallite size of Cu is lower than that of Al.

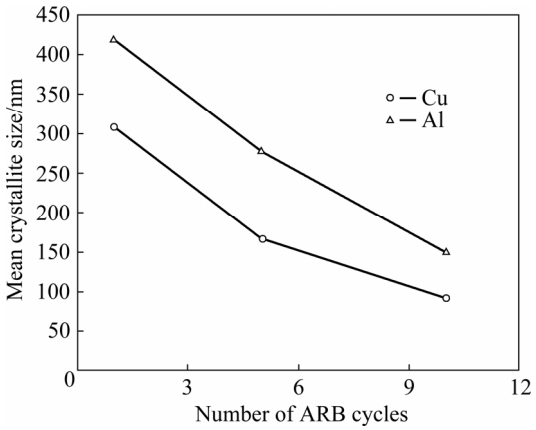

Fig. 4 Variation of mean crystallite size of Cu matrix and Al layers versus number of ARB cycles

At the final ABR cycle, the mean crystallite size of Cu is about 92 nm, whereas the mean crystallite size of Al is about 149 nm. The differences in the mean crystallite size of Cu and Al are attributed to the difference in their stacking fault energy. It has been reported that the stacking fault energies of Cu and Al are 78 and 166 mJ/m^2, respectively [17]. Due to cross slip and dynamic recovery of dislocations during deformation of metals with high stacking fault energy, ultra-fine structure is developed in these metals [17−19]. Both Cu and Al have the face center cubic structure, but Cu has a week tendency to dynamic recovery during the ARB process. Hence, at the final ARB cycle, the nanostructure is extended in the Cu matrix whereas the Al layers have ultra-fine structures. It is noticeable that Ag has the lowest stacking fault energy (30 mJ/m^2) in this composite and is expected to exhibit a nanostructure.

3.2 Mechanical properties

The average bond strength of the constituent layers is an important parameter affecting the mechanical properties of the multilayered composites. The average bond strength between the Cu/Al layers was measured at various rolling deformations, according to Ref. [20] and is shown in Fig. 5.

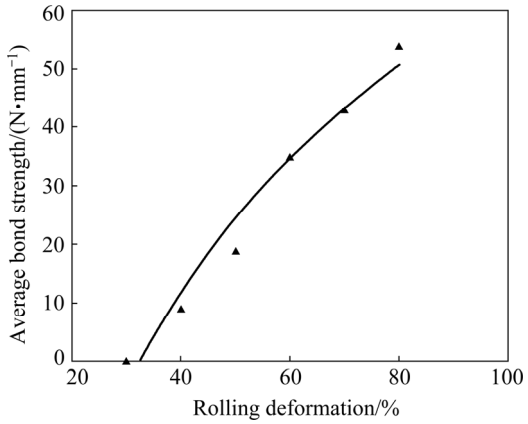

Fig. 5 Average bond strength vs rolling deformation for roll-bonded Cu/Al layers

As it can be seen, this property is increased by increasing the rolling deformation. This is attributed to the fact that the increase of thickness reduction results in the increase of the number of surface cracks and the amount of extruded virgin metals [20].

The engineering stress−strain curves of the multi-layered 70Cu/28Al/2Ag composites fabricated by ARB are shown in Fig. 6.

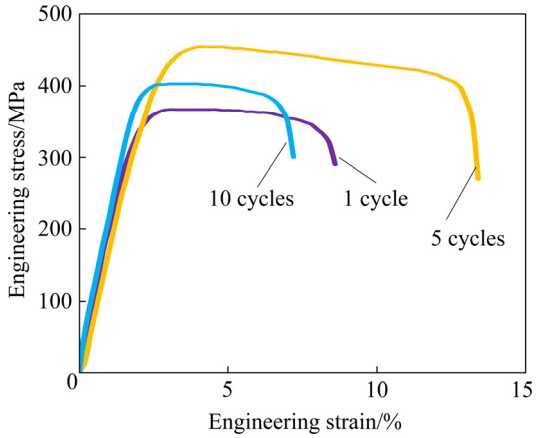

Fig. 6 Engineering stress−strain curves of fabricated multi-layered Cu/Al/Ag composites

The strength of the composites is increased by increasing cycles due to strain hardening (at the initial stages of ARB) and grain refinement (at the final stages of ARB) [20]. However, according to Fig. 6, the strength decreases after 5 cycles. This trend has been previously reported by other researchers [14,21]. For example, MAHDAVIAN et al [14] have shown that the strength of Cu/Al/Zn multi-layered composites decreases after middle cycles. This may be due to different mechanical properties of the constituent layers. It is evident that

the flow properties of Cu are different from those of Al. During the ARB process, the plastic instabilities such as necking and fracture occur as a result of the difference between the flow properties of the Cu and Al layers. Copper as the harder constituent is prone to plastic instability after several ARB cycles. Figure 7 shows the SEM image of the multi-layered Cu/Al/Ag composites.

As it is seen, by increasing ARB cycles, the thickness of the layers decreases whereas their number increases. In the initial cycles, the layers are continuous and their interface has a straight morphology (see Figs. 7(a, b)). By increasing cycles, the interface of the layers gradually tends to a wavy shape. In fact, the Cu hard layers are necked, creating wavy shaped interfaces. From Fig. 7, it is obvious that rupture takes place in the Cu layers after necking, which results in discontinuity in the constituent layers (see Figs. 7(c, d)). It has been reported that the necking and fracture of layers are affected by the following parameters: (1) strain hardening exponents of the constituent layers, (2) strength coefficients of the constituents, and (3) initial thickness ratio of the constituents [14]. As necking extends in the Cu layers, the shear fracture takes place in the Al layers. Additionally, shear bands are created in the composite after middle ARB cycles (see Fig. 7(c)). Thus, the presence of plastic instabilities in the fabricated composites at the final ARB cycles decreases their tensile strength.

The variation in the elongation of the fabricated composites is indicated in Fig. 8.

Similar to strength, the elongation of the composite samples initially increases up to the fifth cycle and then decreases to the final cycle. Generally, the ARB process decreases the ductility of metals compared to the annealed mode [22]. Inadequate bonding and discontinuity between layers and also strain hardening are the factors responsible for this reduction [23,24]. However, the elongation increases by increasing ARB cycles [25]. The increase in elongation is attributed to the decrease of discontinuity between layers and the increase of the bonding area during the ARB process, as indicated in Fig. 9.

In Fig. 9, the fracture surface of the composite samples after the tensile tests is shown. Considering

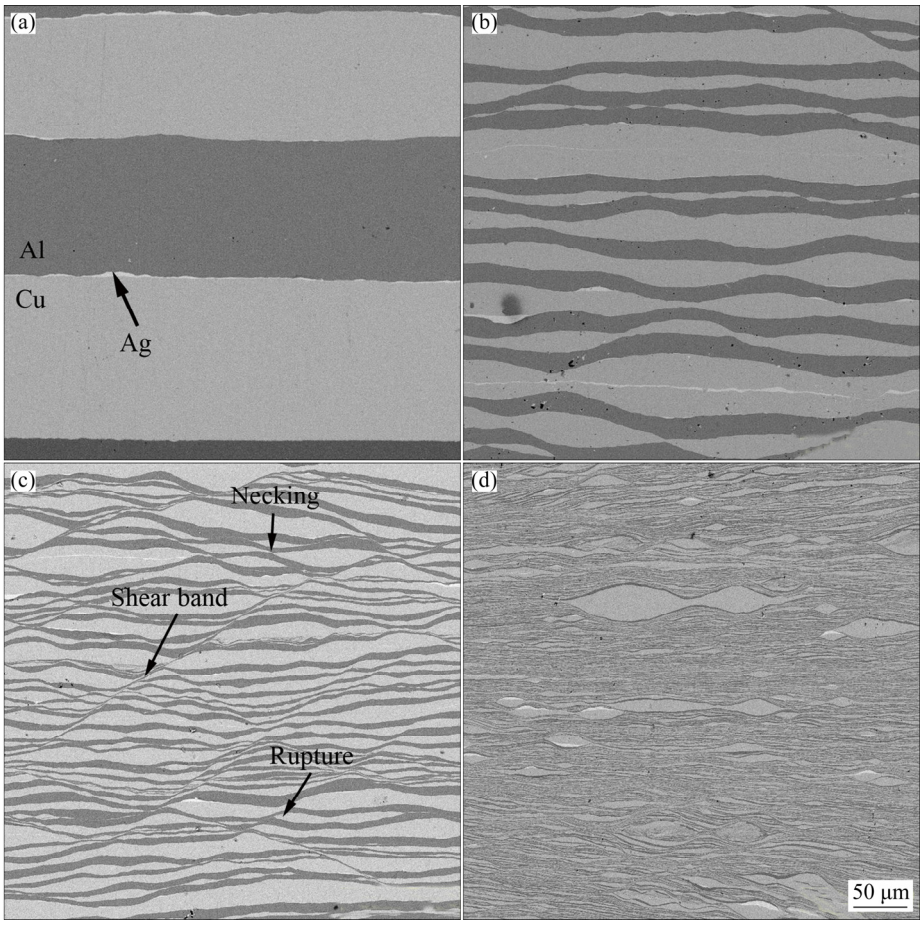

Fig. 7 Cross-sectional SEM micrographs of composites fabricated by different cycles of ARB: (a) 1; (b) 4; (c) 8; (d) 10

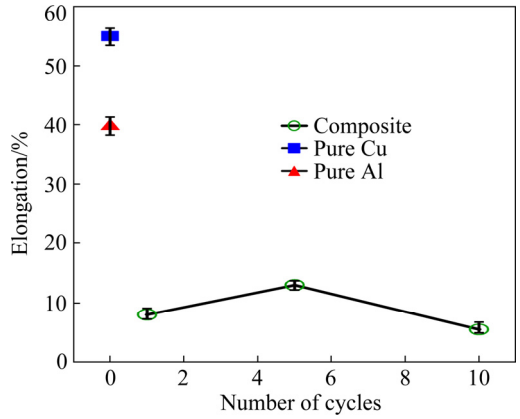

Fig. 8 Variation in elongation of fabricated composite

the flat areas of the fracture surfaces of the samples prepared by ARB after the first cycle, it is obvious that a brittle fracture happens in these samples (Fig. 9(a)). Some discontinuities are also seen between the interfaces of the layers. This confirms the decrease in elongation at the beginning of the ARB process. According to Fig. 9(b), the discontinuities decrease after 5 cycles, which results in the increase of elongation. But after the final ARB cycle, the plastic instabilities decrease the elongation.

Figure 10 shows the variation in the microhardness of the layers (Al and Cu) and fabricated composite versus ARB cycles.

In the initial ARB cycles, the layers are thick enough to measure their microhardness. However, after 5 cycles, the layers become too thin to measure it; hence, the microhardness of the composites was reported for them. As it can be seen, unlike strength and elongation, the microhardness of the composites is increased by increasing the cycles. This shows that the microhardness does not depend on the plastic instabilities (necking, rupture, and fracture of the layers).

3.3 Strength prediction

High strength is a desirable property for multi-layered metal composites. The strength of the multi-layered metal composites is higher than that of their single materials due to some strengthening mechanisms. Strengthening mechanisms in multi-layered metal composites are as follows: (1) dislocation strengthening (strain hardening), (2) Hall−Petch strengthening or grain refinement, (3) back stress strengthening, and (4) thermal expansion dislocation strengthening [9,23,26,27].

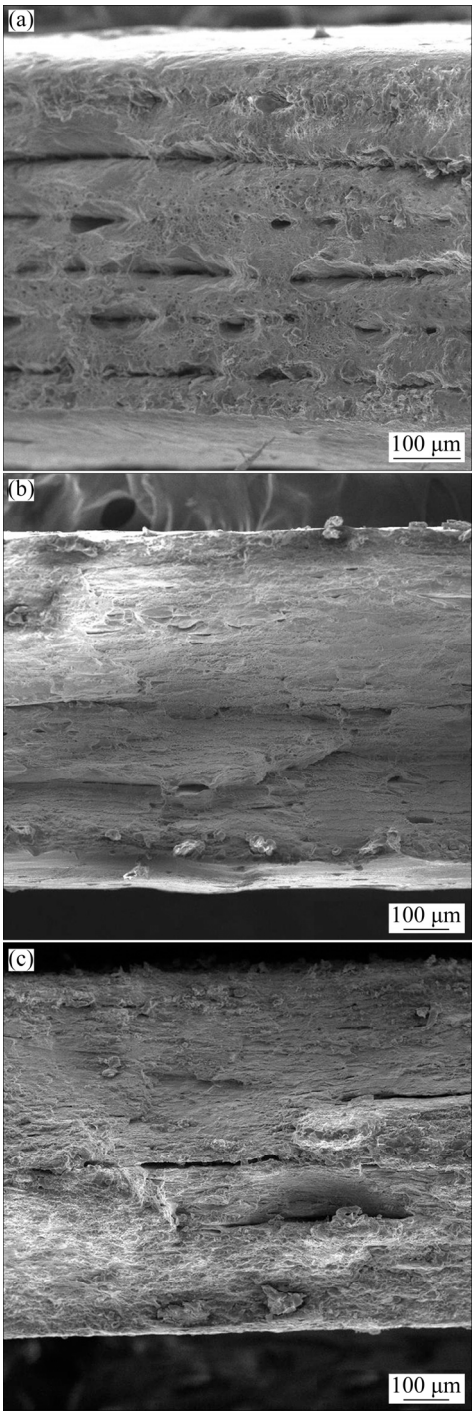

Fig. 9 Fracture surface morphologies of composite samples fabricated by different cycles of ARB after tensile tests: (a) 1; (b) 5; (c) 10

In the initial ARB cycles, many dislocations are generated in the samples. The dislocations interact together and incidental dislocation boundaries (IDBs) are created due to the trapping of dislocations. The increase of strength due to this event is known as dislocation strengthening or strain hardening. The strength raised by strain hardening can be estimated by the expression as

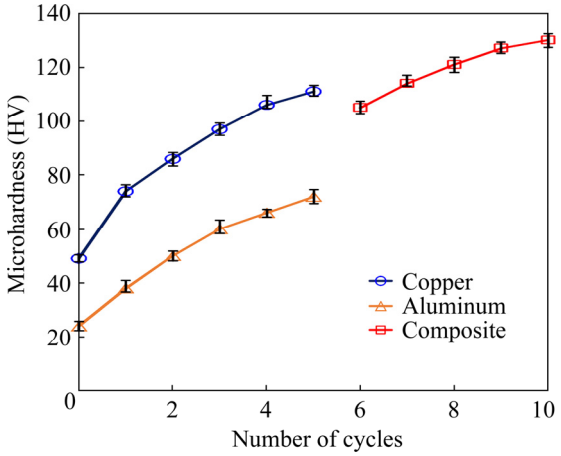

Fig. 10 Variation of micro-hardness of pure metals and fabricated composites

follows [28]:

$$\sigma_{ds}=M\alpha Gb\sqrt{\rho} \tag{2}$$

where M is the Taylor factor (3.06), G is the shear modulus, α is constant, b is the magnitude of Burger vector, and ρ is the dislocation density.

During the ARB process, grain refinement occurs and, based on material properties, ultra-fine or nanometric grains extend in the samples [28−30]. The decrease in grain size increases the strength of the composite samples, according to the Hall−Petch equation [31,32]:

$$\sigma_{HP}=\sigma_0+\frac{K_{HP}}{\sqrt{D}} \tag{3}$$

where σ_0 is the friction stress, K_{HP} is the Hall−Petch slope and D is the average mean crystallite size.

Due to the difference between the thermal expansion of copper and aluminum layers during quenching of the composites after each ARB cycle, some dislocations are generated. The dislocation density due to the difference between the thermal expansions can be calculated by the following equation [27]:

$$\rho_{Th}=12\Delta T\Delta CV/(bl) \tag{4}$$

where ΔT is the temperature change, ΔC is the thermal mismatch, V is the volume fraction of the reinforcement, and l is the thickness of the reinforcement(s). The strength can be estimated by [27]

$$\sigma_{bs}=\alpha Gb\sqrt{\rho_{Th}} \tag{5}$$

A mechanical incompatibility between copper and aluminum is created during the ARB process due to the difference in their flow properties, strength, grain size, and stacking fault energy [10]. Since copper and aluminum layers are forced together during ARB process, a strain gradient is necessarily generated in their interface to fit the different strains in these layers. In this case, geometrically necessary dislocations (GNDs) are created near the interfaces of copper and aluminum layers [10]. By increasing the strain (increasing the number of ARB cycles), GNDs are increased and GNDs pile-up occurs in the interfaces of the Cu and Al layers. The dislocation pile-up in the interface of the Cu and Al layers produces a back stress [10]. Hence, a stress field is produced, which can inhibit dislocation emission from their source. More flow stress is thereby required to overcome this field, which is called “back stress strengthening”. The value of the back stress is proportion to the density of GNDs (ρ_{GNDs}). MA et al [9] and GAO [33] proposed a simple relation to determine the density of GNDs as follows:

$$\rho_{GNDs}=\frac{2\theta}{lb} \tag{6}$$

where θ is the local misorientation, and b=0.286 nm for aluminum. The strength due to the back stress can be estimated by the following expression:

$$\sigma_{bs}=\alpha Gb\sqrt{\rho_{GNDs}} \tag{7}$$

where α=0.5−1.

The final strength of the fabricated multi-layered composites can be estimated by following equation:

$$\sigma_C=\sigma_{ds}+\sigma_{HP}+\sigma_{Th}+\sigma_{bs} \tag{8}$$

Replacing each expression in Eq. (8), the strength of the composites is expressed by

$$\sigma_C=M\alpha Gb\sqrt{\rho_{ds}}+\sigma_0+\frac{K_{HP}}{\sqrt{D}}+\alpha Gb\sqrt{\rho_{Th}}+\alpha Gb\sqrt{\rho_{GNDs}} \tag{9}$$

The terms σ_{bs} and ρ_{Th} can be considered as the portions of strain hardening strengthening. Hence, Eq. (9) is changed as follows:

$$\sigma_C=M\alpha Gb\sqrt{\rho}+\sigma_0+\frac{K_{HP}}{\sqrt{D}} \tag{10}$$

where $\rho=\rho_{ds}+\rho_{bs}+\rho_{Th}$.

The amount of Ag in the fabricated composites is so low that the effect of this insoluble species on the increase of strength is considered to be negligible. Since the flow properties and stacking fault energy of copper and aluminum are different, each constituent has different contributions to strain hardening and Hall−Petch strengthening. Using the rule of mixture, Eq. (10) is changed as follows:

$$\sigma_C = V_{Cu}(\sigma_0 + M\alpha Gb\sqrt{\rho} + \frac{K_{HP}}{\sqrt{D}})_{Cu} + V_{Al}(\sigma_0 + M\alpha Gb\sqrt{\rho} + \frac{K_{HP}}{\sqrt{D}})_{Al} \quad (11)$$

where V_{Cu} and V_{Al} are the volume fractions of copper and aluminum, respectively.

It should be noted that plastic instability due to the difference between the flow properties of the constituents decreases the tensile strength of the fabricated composites after middle cycles. The amount of this reduction is approximately equal to the yield strength of the matrix (σ_{ym}). Hence, Eq. (11) is changed as follows:

$$\sigma_C = V_{Cu}(\sigma_0 + M\alpha Gb\sqrt{\rho} + \frac{K_{HP}}{\sqrt{D}})_{Cu} + V_{Al}(\sigma_0 + M\alpha Gb\sqrt{\rho} + \frac{K_{HP}}{\sqrt{D}})_{Al} - \sigma_{ym} \quad (12)$$

It is noticeable that σ_{ym} is considered from the cycle in which the plastic instabilities of the fabricated composite start.

The parameters presented in Eq. (12) were extracted from references [34,35] and listed in Table 2.

Table 2 Some properties of copper and aluminum layers

Material	σ_{uts}/ MPa	G/ GPa	b/ nm	K_{HP}/ (MPa·m$^{1/2}$)	V/ %
Copper	205	45	0.256	0.14	70
Aluminum	90	26	0.286	0.04	28

The mean crystallite size and dislocation density of the fabricated composites were also determined by the XRD data and tabulated in Table 3.

Replacing the data given in Tables 2 and 3 in Eq. (12), the strength of the fabricated composites can be calculated. Both the calculated and experimental tensile strength of the fabricated multi-layered composites are shown in Fig. 11.

Table 3 Mean crystallite size and dislocation density of composites

Material	Number of cycles	mean crystallite size/nm	Dislocation density/m^{-2}
Copper	1	308	1.0×10^{14}
	5	167	2.5×10^{14}
	10	92	1.8×10^{14}
Aluminum	1	420	4.1×10^{13}
	5	278	8.3×10^{13}
	10	149	7.1×10^{13}

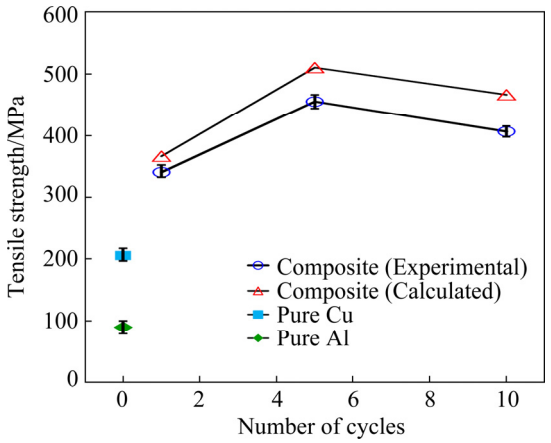

Fig. 11 Calculated and experimental tensile strength of fabricated multi-layered composites

It is shown that there is a good agreement between the calculated and experimental values. By comparing the calculated and measured tensile strength values, it is evident that there is a difference between the calculated and experimental tensile strength values. The calculated data are higher than the experimental data. The most important reasons for this difference can be described as follows.

(1) For the calculation of tensile strength, the mean crystallite size and dislocation density calculated by the XRD analyses were used in Eq. (12), whereas the XRD method is not accurate to do so [36]. It has been reported that the mean crystallite size of an ARBed sample measured by the XRD method is smaller than the actual value [37,38].

(2) Some defects between layers are created during the ARB process, which are not considered in Eq. (12). These defects can include voids, insufficient bonding between the layers, and agglomeration of the Ag powders, which decreases the composites strength in practice due to the stress

concentration. From the above discussion, it can be concluded that if the grain size and dislocation density are determined in a suitable accuracy, Eq. (12) can properly predict the strength of the multi-layered composites fabricated by the ARB process.

3.4 Electrical conductivity

ARB as a severe plastic deformation route can affect the electrical conductivity of the processed materials [39]. Figure 12 shows the electrical conductivity of the as-received pure Cu, pure Al, pure Ag and the fabricated Cu/Al/Ag composites. As it can be seen, the electrical conductivity decreases slightly by increasing the number of ARB cycles. However, the decrease in electrical conductivity at the final ARB cycles is larger than that of the initial ARB cycles. It has been reported that electrical conductivity depends on several microstructural parameters, such as solute atoms (solid solution), second phase particles, grain boundaries, dislocations, and vacancies [39]. Among these parameters, solute atoms and second phase particles have significant effects on electrical conductivity, while the effect of the others is negligible [39]. In the present work, by increasing the number of ARB cycles, the density of dislocations and the number of grain boundaries increase, resulting in the slight decrease of electrical conductivity. In fact, the presence of dislocations causes the scattering of electrons, which leads to the decrease of electrical conductivity [40].

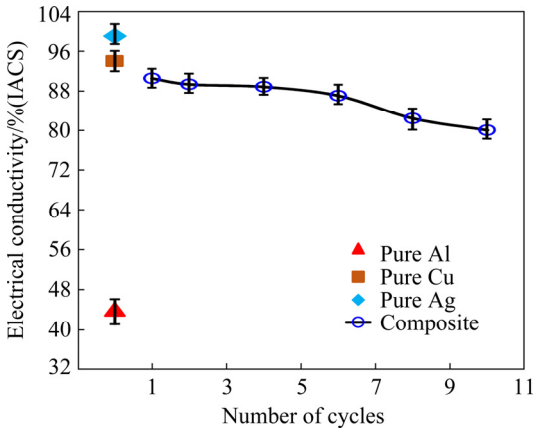

Fig. 12 Electrical conductivity of as-received pure Cu, pure Al and fabricated Cu/Al/Ag composites

As it can be seen in Fig. 12, the variation of electrical conductivity in the final ARB cycles is different from the initial cycles. This is attributed to the presence of aluminum islands on the surface in the vicinity of the copper matrix. As indicated in Fig. 1, the sequence stacking of the layers in the composite samples is Cu/Al/Cu/Al/Cu/Al/Cu. It is obvious that at the beginning of the process, outer layers of the fabricated composite samples are copper. Figure 13 shows the optical micrograph of the fabricated Cu/Al/Ag samples. In the initial ARB cycles, copper remains on the surface as the outer layer (see Figs. 13(a, b)). Therefore, in the initial cycles, the measured electrical conductivity is related to copper and the effect of aluminum is negligible. The thickness of copper layers decreases

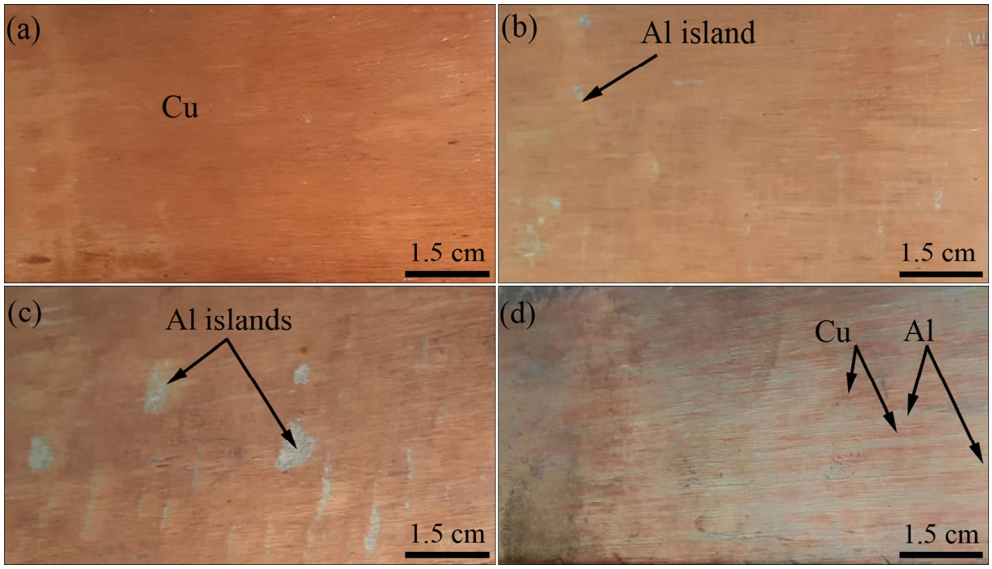

Fig. 13 Optical images of Cu/Al/Ag composites fabricated by different cycles of ARB: (a) 1; (b) 5; (c) 7; (d) 10

gradually, so that Al layers can reach the surface of the composites at final cycles (see Figs. 13(c, d)). The presence of Al islands on the surface decreases the electrical conductivity of the samples due to the lower electrical conductivity of aluminum compared to copper.

4 Conclusions

(1) Plastic instabilities such as necking and fracture of the constituent layers were observed in the microstructure.

(2) Both the tensile strength and ductility of the prepared composites increased with the ARB cycles up to middle cycles and then dropped at the final cycle.

(3) The suitable agreement between the calculated and experimental tensile strength data showed that the model used for the strength prediction is dependable.

(4) The ARB process did not significantly change the electrical conductivity of the Cu/Al/Ag composites in the initial cycles, while increased its strength significantly.

References

[1] WANG L, DU Q L, LI C, CUI X H, ZHAO X, YU H L. Enhanced mechanical properties of lamellar Cu/Al composites processed via high-temperature accumulative roll bonding [J]. Transactions of Nonferrous Metals Society of China, 2019, 29: 1621−1630.

[2] CHENG W J, LIU Y, ZHAO D P, LIU B, TAN Y, WANG X G, TANG H C. Crack propagation behavior of inhomogeneous laminated Ti−Nb metal−metal composite [J]. Transactions of Nonferrous Metals Society of China, 2019, 29: 1882−1888.

[3] LI X B, ZU G Y, WANG P. Microstructural development and its effects on mechanical properties of Al/Cu laminated composite [J]. Transactions of Nonferrous Metals Society of China, 2015, 25: 36−45.

[4] JOVANOVIĆ M T, LIĆI N, CVIJOVIĆ-ALAGIĆ I, MAKSIMOVIĆ V, ZEC S. Multilayer aluminum composites prepared by rolling of pure and anodized aluminum foils [J]. Transactions of Nonferrous Metals Society of China, 2017, 27: 1907−1919.

[5] HOKAMOTO K, CHIBA A, FUJITA M, IZUMA T. Single-shot explosive welding technique for the fabrication of multilayered metal base composites: Effect of welding parameters leading to optimum bonding condition [J]. Composite Engineering, 1995, 5: 1069−1079.

[6] LAZURENKO D B, MALI V A, ANISIMOV A G, YARTSEV P S, LAGEREVA D I, SHEVTSOVA L I. The structural particularities of multilayered metal-intermetallic composites fabricated by the spark plasma sintering technology [J]. Advanced Materials Research, 2014, 1040: 800−804.

[7] ALIZADEH M, SALAHINEJAD E. Processing of ultrafine-grained aluminum by cross accumulative roll-bonding [J]. Materials Science and Engineering A, 2014, 595: 131−134.

[8] SAITO Y, UTSUNOMIYA H, TSUJI N, SAKAI T. Novel ultra-high straining process for bulk materials—Development of the accumulative roll-bonding (ARB) process [J]. Acta Materialia, 1999, 47: 579−583.

[9] MA X, HUANG C, MOERING J, RUPPERT M, HÖPPEL H W, GÖKEN M, NARAYAN J, ZHU Y. Mechanical properties of copper/bronze laminates: Role of interfaces [J]. Acta Materialia, 2016, 116: 43−52.

[10] MO T Q, CHEN Z J, CHEN H, HU C, HE W J, LIU Q. Multiscale interfacial structure strengthening effect in Al alloy laminated metal composites fabricated by accumulative roll bonding [J]. Materials Science and Engineering A, 2019, 766: 138354.

[11] GAO H T, LIU X H, QI J L, AI Z R, LIU L Z. Microstructure and mechanical properties of Cu/Al/Cu clad strip processed by the powder-in-tube method [J]. Journal of Materials Processing Technology, 2018, 251: 1−11.

[12] RAHMATABADI D, MOHAMMADI B, HASHEMI R, SHOJAEE T. An experimental study of fracture toughness for nano/ultrafine grained Al5052/Cu multilayered composite processed by accumulative roll bonding [J]. Journal of Manufacturing Science and Engineering, 2018, 140: 101001.

[13] ALIZADEH M, DASHTESTANINEJAD M K. Development of Cu-matrix, Al/Mn-reinforced, multilayered composites by accumulative roll bonding (ARB) [J]. Journal of Alloys and Compounds, 2018, 723: 674−682.

[14] MAHDAVIAN M M, GHALANDARI L, REIHANIAN M. Accumulative roll bonding of multilayered Cu/Zn/Al: An evaluation of microstructure and mechanical properties [J]. Materials Science and Engineering A, 2013, 579: 99−107.

[15] ALIZADEH M, AVAZZADEH M. Evaluation of Cu−26Zn−5Al shape memory alloy fabricated by accumulative roll bonding process [J]. Materials Science and Engineering A, 2019, 757: 88−94.

[16] WILLIAMSON G K, HALL W H. X-ray line broadening from filed aluminium and wolfram [J]. Acta Metallurgica, 1953, 1: 22−31.

[17] HUMPHREYS F H, HATHERLY M. Recrystallization and related annealing phenomena, [M]. 2nd ed. Amsterdam: Elsevier, 2004.

[18] YAZDANI A, SALAHINEJAD E, MORADGHOLI J, HOSSEINI M. A new consideration on reinforcement distribution in the different planes of nanostructured metal matrix composite sheets prepared by accumulative roll bonding (ARB) [J]. Journal of Alloys and Compounds, 2011, 509: 9562−9564.

[19] YAGHTIN A H, SALAHINEJAD E, KHOSRAVIFARD A. Processing of nanostructured metallic matrix composites by a modified accumulative roll bonding method with structural and mechanical considerations [J]. International Journal of Minerals, Metallurgy, and Materials, 2012, 19: 951−956.

[20] ALIZADEH M, SHAKERY A, SALAHINEJAD E. Aluminum-matrix composites reinforced with E-glass fibers by cross accumulative roll bonding process [J]. Journal of Alloys and Compounds, 2019, 804: 450−456.

[21] WU K, CHANG H, MAAWAD E, GAN W N, BROKMEIER H G, ZHENG M Y. Microstructure and mechanical properties of the Mg/Al laminated composite fabricated by accumulative roll bonding (ARB) [J]. Materials Science and Engineering A, 2010, 527: 3073−3078.
[22] ALIZADEH M, PAYDAR M H. High-strength nanostructured Al/B_4C composite processed by cross-roll accumulative roll bonding [J]. Materials Science and Engineering A, 2012, 538: 14−19.
[23] ALIZADEH M, BENI H A. Strength prediction of the ARBed Al/Al_2O_3/B_4C nano-composites using Orowan model [J]. Materials Research Bulletin, 2014, 59: 290−294.
[24] TAYYEBI M, RAHMATABADI D, ADHAMI M, HASHEMI R. Influence of ARB technique on the microstructural, mechanical and fracture properties of the multilayered Al1050/Al5052 composite reinforced by SiC particles [J]. Journal of Materials Research and Technology, 2019, 8: 4287−4301.
[25] ALIZADEH M, PAYDAR M H. Fabrication of nanostructure Al/SiC_P composite by accumulative roll-bonding (ARB) process [J]. Journal of Alloys and Compounds, 2010, 492: 231−235.
[26] ALIZADEH M. Strengthening mechanisms in particulate Al/B_4C composites produced by repeated roll bonding process [J]. Journal of Alloys and Compounds, 2011, 509: 2243−2247.
[27] MILLER W S, HUMPHREYS F J. Strengthening mechanisms in particulate metal matrix composites [J]. Scripta Metallurgica et Materialia, 1991, 25: 33−38.
[28] REIHANIAN M, EBRAHIMI R, TSUJI N, MOSHKSAR M M. Analysis of the mechanical properties and deformation behavior of nanostructured commercially pure Al processed by equal channel angular pressing (ECAP) [J]. Materials Science and Engineering A, 2008, 473: 189−194.
[29] PEREZ-PRADO M T, RUANO O A. Grain refinement of Mg−Al−Zn alloys via accumulative roll bonding [J]. Scripta Materialia, 2004, 51: 1093−1097.
[30] SCHMIDT C W, KNEIKE C, MAIER V, HÖPPEL H W, PEUKERT W, GÖKEN M. Accelerated grain refinement during accumulative roll bonding by nanoparticle reinforcement [J]. Scripta Materialia, 2011, 64: 245−248.
[31] ARMSTRONG R W, BALASUBRAMANIAN N. Unified Hall−Petch description of nano-grain nickel hardness, flow stress and strain rate sensitivity measurements [J]. AIP Advances, 2017, 7: 85010.
[32] LI C L, MEI Q S, LI J Y, CHEN F, MA Y, MEI X M. Hall−Petch relations and strengthening of Al−ZnO composites in view of grain size relative to interparticle spacing [J]. Scripta Materialia, 2018, 153: 27−30.
[33] GAO H. Mechanism-based strain gradient plasticity I. Theory [J]. Journal of Mechanics and Physics of Solids, 1999, 47: 1239−1263.
[34] HANSEN N. Hall−Petch relation and boundary strengthening [J]. Scripta Materialia, 2004, 51: 801−806.
[35] THOMPSON A W, BACKOFEN W A. Production and mechanical behavior of very fine-grained copper [J]. Metallurgical and Materials Transactions B, 1971, 2: 2004−2005.
[36] ZHANG Z, ZHOU F, LAVERNIA E J. On the analysis of grain size in bulk nanocrystalline materials via X-ray diffraction [J]. Metallurgical and Materials Transactions A, 2003, 34: 1349−1355.
[37] HORITA Z, LANGDON T G. Microstructures and microhardness of an aluminum alloy and pure copper after processing by high-pressure torsion [J]. Materials Science and Engineering A, 2005, 410: 422−425.
[38] KHAN A S, FARROKH B, TAKACS L. Compressive properties of Cu with different grain sizes: Sub-micron to nanometer realm [J]. Journal of Materials Science, 2008, 43: 3305−3313.
[39] LIPINSKA M, BAZARNIK P, LEWANDOWSKA M. The influence of severe plastic deformation processes on electrical conductivity of commercially pure aluminium and 5483 aluminium alloy [J]. Archives of Civil and Mechanical Enigineering, 2016, 16: 717−723.
[40] GHALANDARI L, MOSHKSAR M M. High-strength and high-conductive Cu/Ag multilayer produced by ARB [J]. Journal of Alloys and Compounds, 2010, 506: 172−178.

累积叠轧焊多层铜基复合材料的强度预测

P. SEIFOLLAHZADEH, Morteza ALIZADEH, M. R. ABBASI

Department of Materials Science and Engineering, Shiraz University of Technology,
Modarres Blvd., 71557-13876, Shiraz, Iran

摘　要：评价用累积叠轧焊(ARB)制备纳米结构 Cu/Al/Ag 多层复合材料的可行性，分析该复合材料的拉伸性能和电导率。利用强化机制和从 X 射线衍射获取的结构参数建立理论模型预测复合材料的抗拉强度。结果表明，随着 ARB 的进行，实验和计算得到的抗拉强度均有所提高，在第 5 个 ARB 循环时达到最大值，分别为 450 MPa 和 510 MPa。在初始 ARB 循环后，电导率略有下降；随着 ARB 循环次数的继续增加，电导率的下降幅度增大。总之，用 ARB 制备这类多层纳米复合材料具有优势，所建立的模型可准确预测材料的抗拉强度。

关键词：多层复合材料；累积叠轧焊；强度预测；硬度；X 射线衍射

(Edited by Bing YANG)